Electronic Supplementary Material (ESI) for Catalysis Science & Technology.

Supplementary Information

Grass-like Ni_xSe_y nanowire arrays shelled with NiFe LDH nanosheets as a 3D hierarchical core-shell electrocatalyst for efficient upgrading of biomass-derived 5-hydroxymethylfurfural and furfural

Yan Zhong[a], Ru-Quan Ren[a], Jian-Bo Wang[a], Yi-Yi Peng[a], Qiang Li[*b] and Yong-Ming Fan[*a]

a. Key Laboratory of Lignocellulosic Chemistry, College of Material Science and Technology, Beijing Forestry University, Beijing, 100083, China.

b. College of Science, Beijing Forestry University, Beijing 100083, China.

*. Corresponding Author. E-mail: fanym@bjfu.edu.cn; liqiang@bjfu.edu.cn.

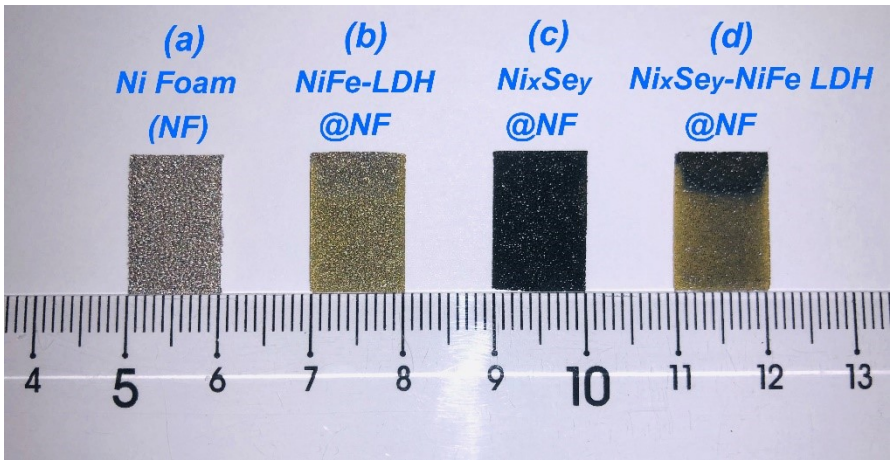

Figure S1 Digital images of as-prepared electrodes: (a)Ni foam; (b)NiFe-LDH@NF; (c)Ni_xSe_y@NF; (d)Ni_xSe_y-NiFe LDH@NF.

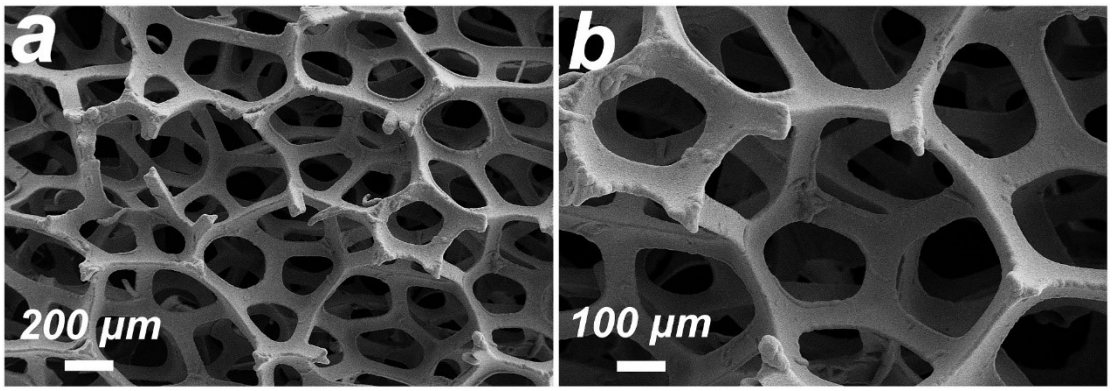

Figure S2 SEM images of commercial Ni foam at different magnifications.

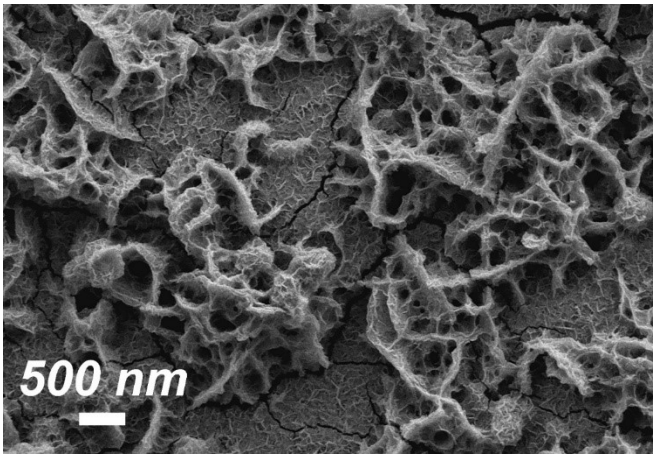

Figure S3 SEM image of NiFe-LDH nanosheets on Ni foam.

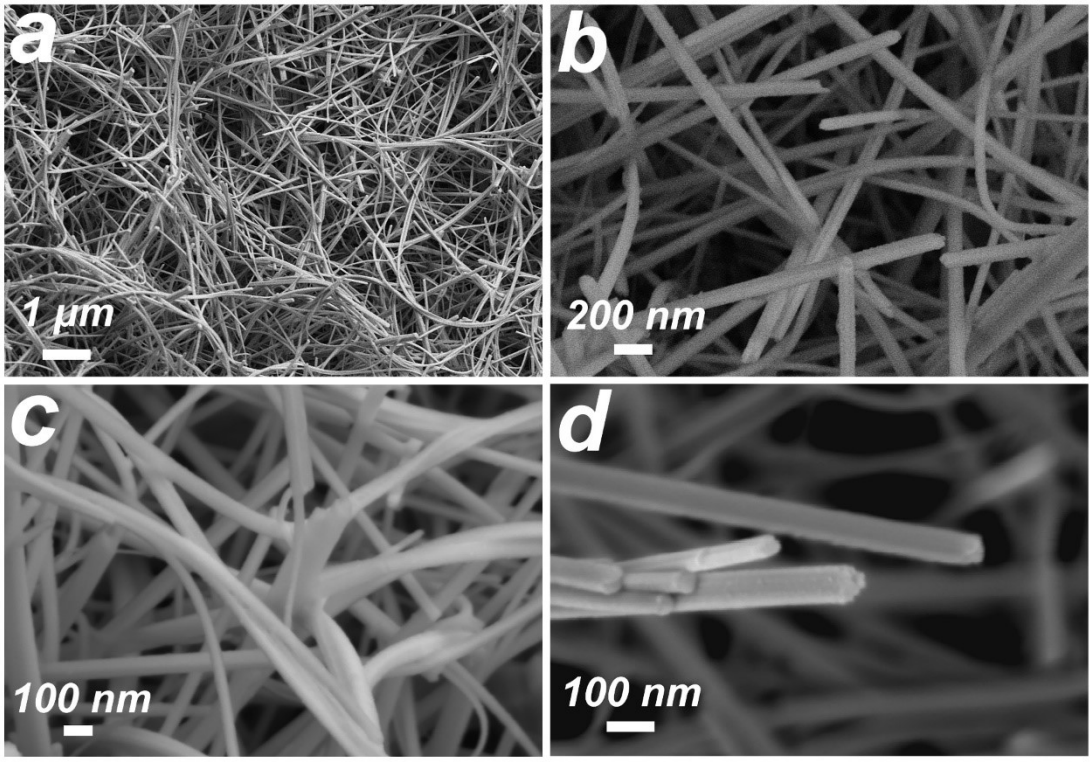

Figure S4 SEM images of Ni_xSe_y@NF nanowire arrays at low and high magnifications.

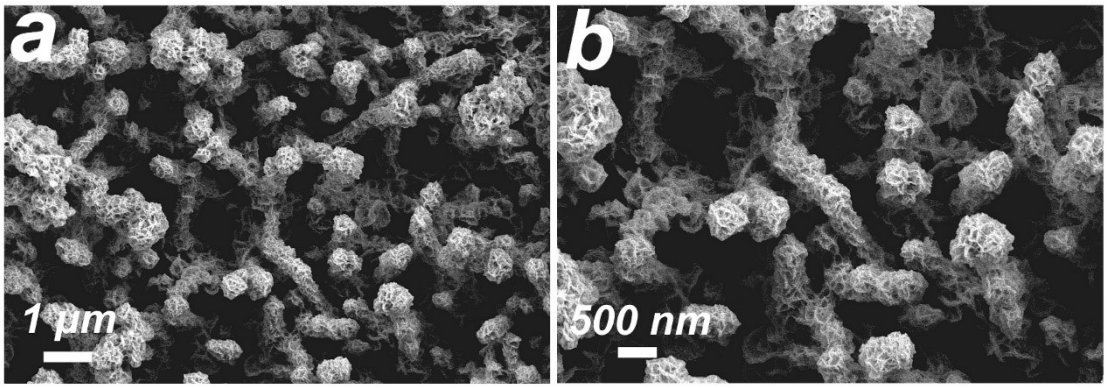

Figure S5 SEM images of Ni_xSe_y-NiFe LDH@NF at low and high magnifications.

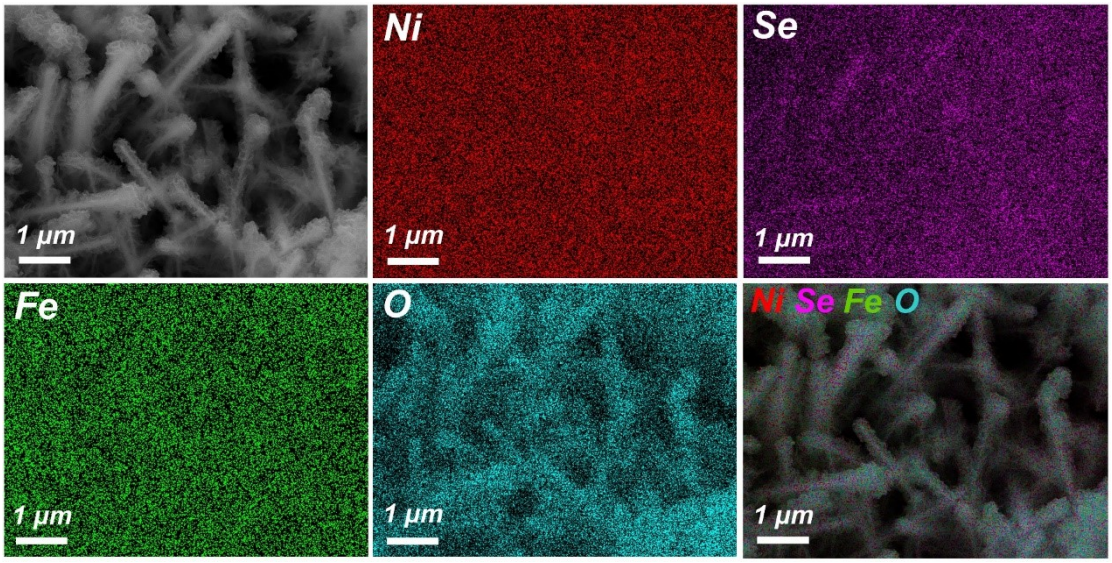

Figure S6 SEM elemental mapping images of Ni_xSe_y-NiFe LDH@NF electrode.

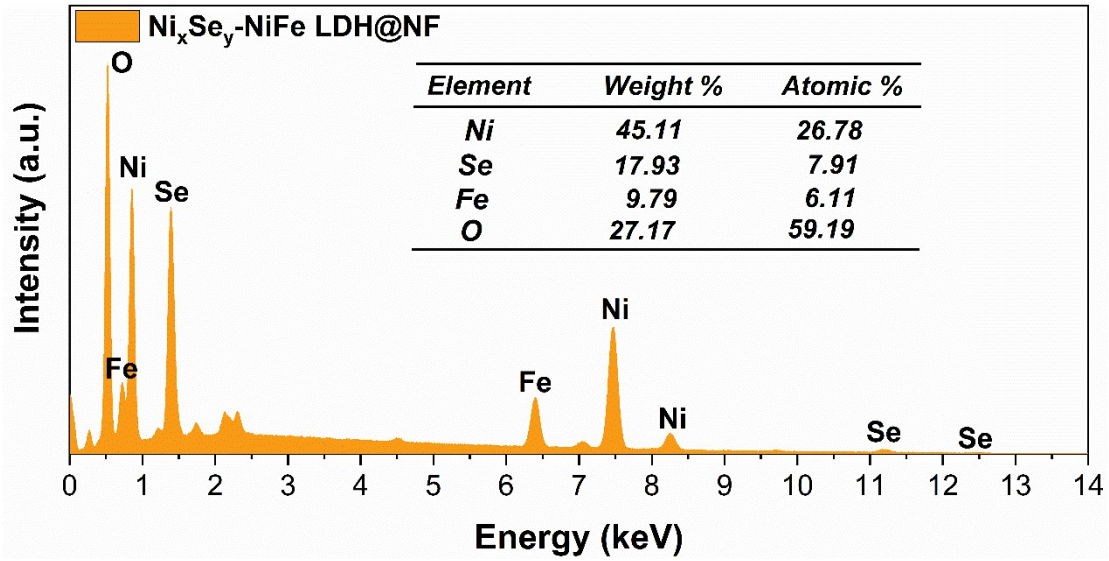

Figure S7 Energy-dispersive X-ray (EDX) spectrum of Ni_xSe_y-NiFe LDH@NF under SEM mode.

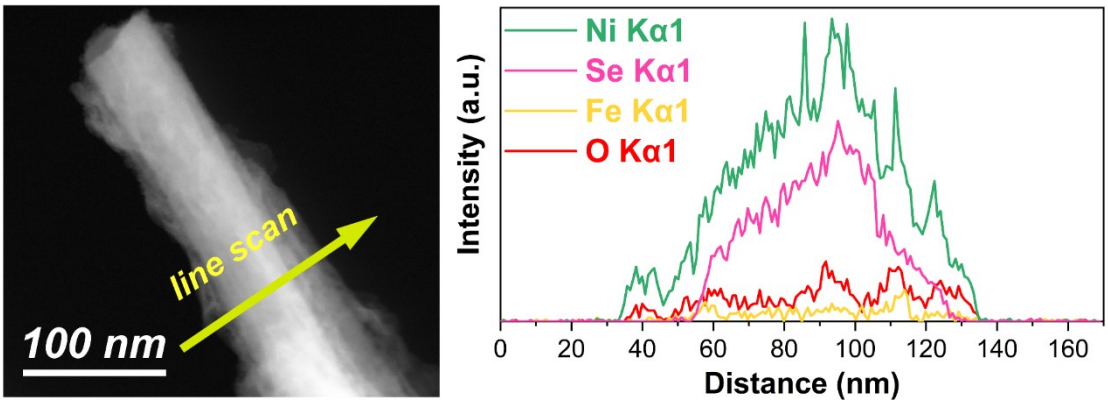

Figure S8 TEM line-scan analysis of Ni_xSe_y-NiFe LDH core-shell structure.

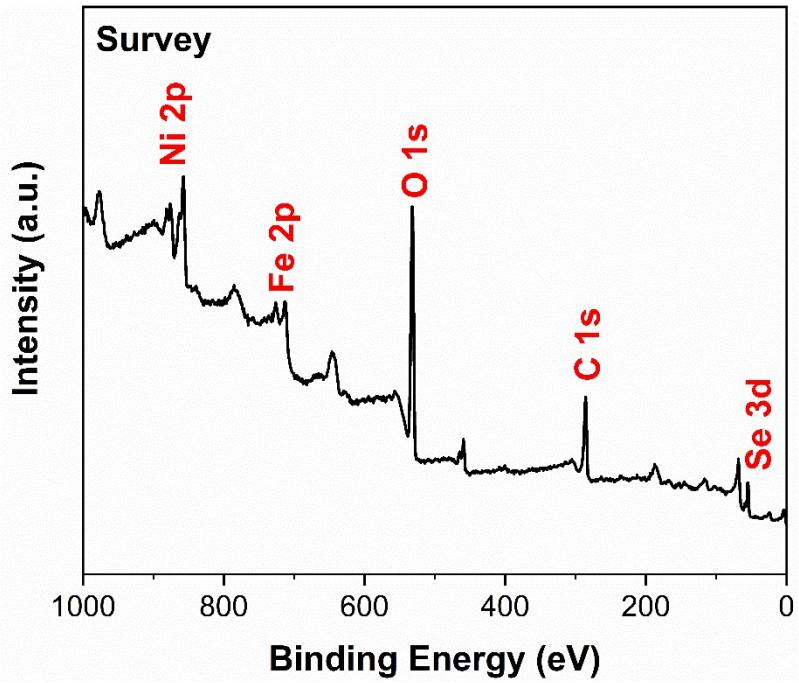

Figure S9 XPS full survey spectrum of Ni_xSe_y-NiFe LDH@NF.

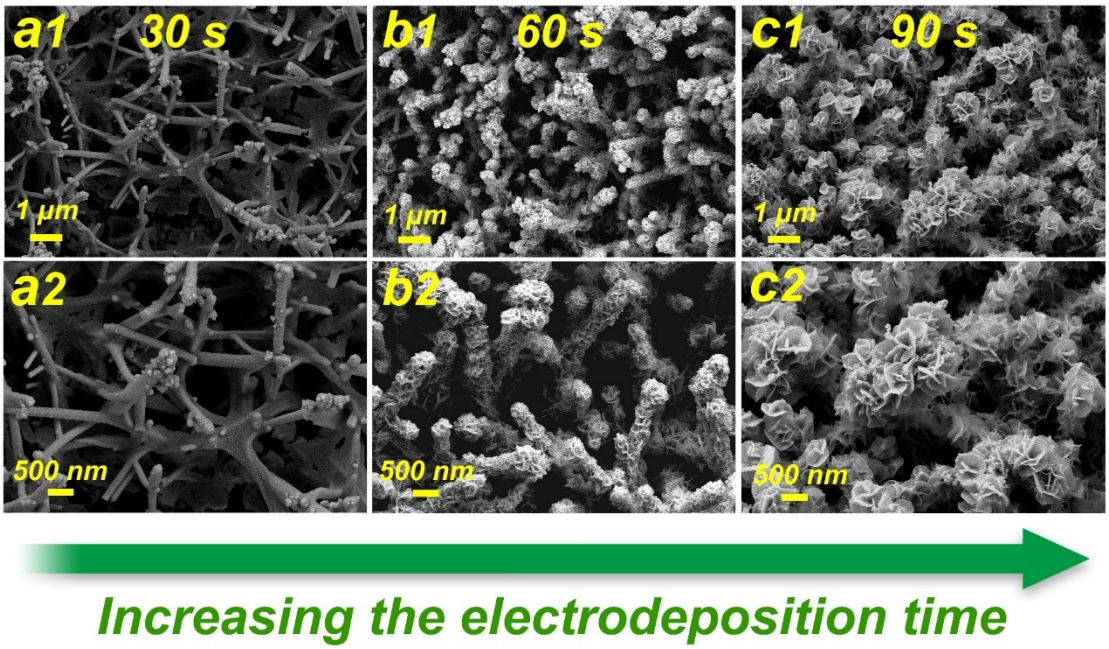

Figure S10 SEM images of (a1,a2) Ni_xSe_y-NiFe LDH@NF-30s; (b1,b2) Ni_xSe_y-NiFe LDH@NF-60s, and (c1,c2) Ni_xSe_y-NiFe LDH@NF-90s at low and high magnifications.

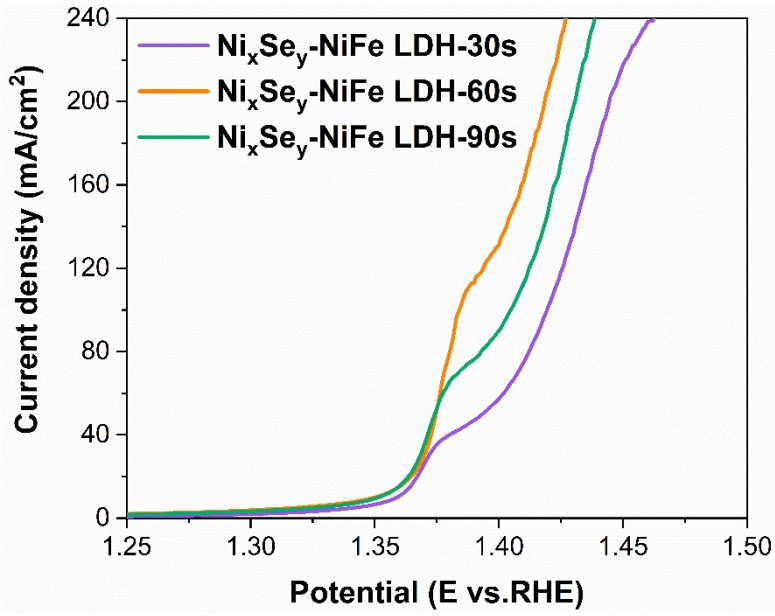

Figure S11 Linear sweep voltammetry curves of Ni_xSe_y-NiFe LDH@NF-30s; Ni_xSe_y-NiFe LDH@NF-60s; Ni_xSe_y-NiFe LDH@NF-90s in 1M KOH with HMF.

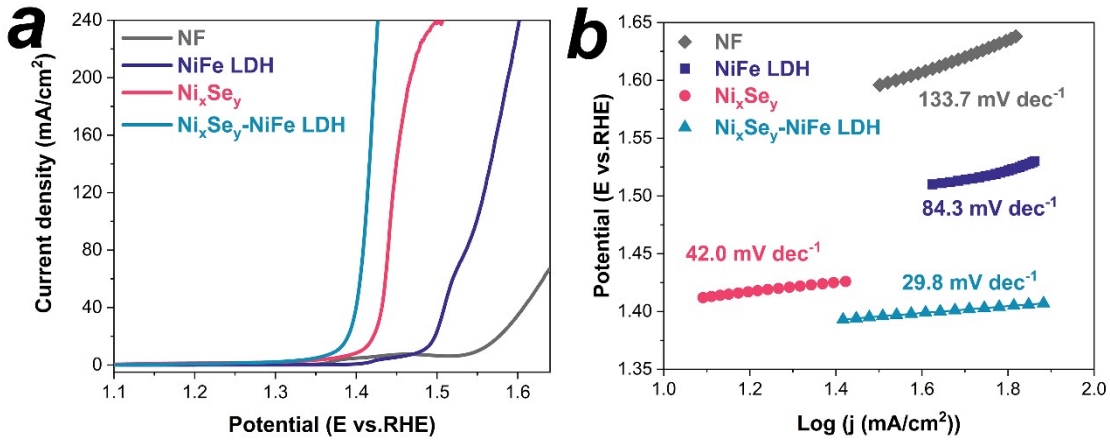

Figure S12 (a) Linear sweep voltammetry (LSV) curves of NF; NiFe LDH@NF; Ni_xSe_y@NF and Ni_xSe_y-NiFe LDH@NF for FUR oxidation and (b) the corresponding Tafel Plots.

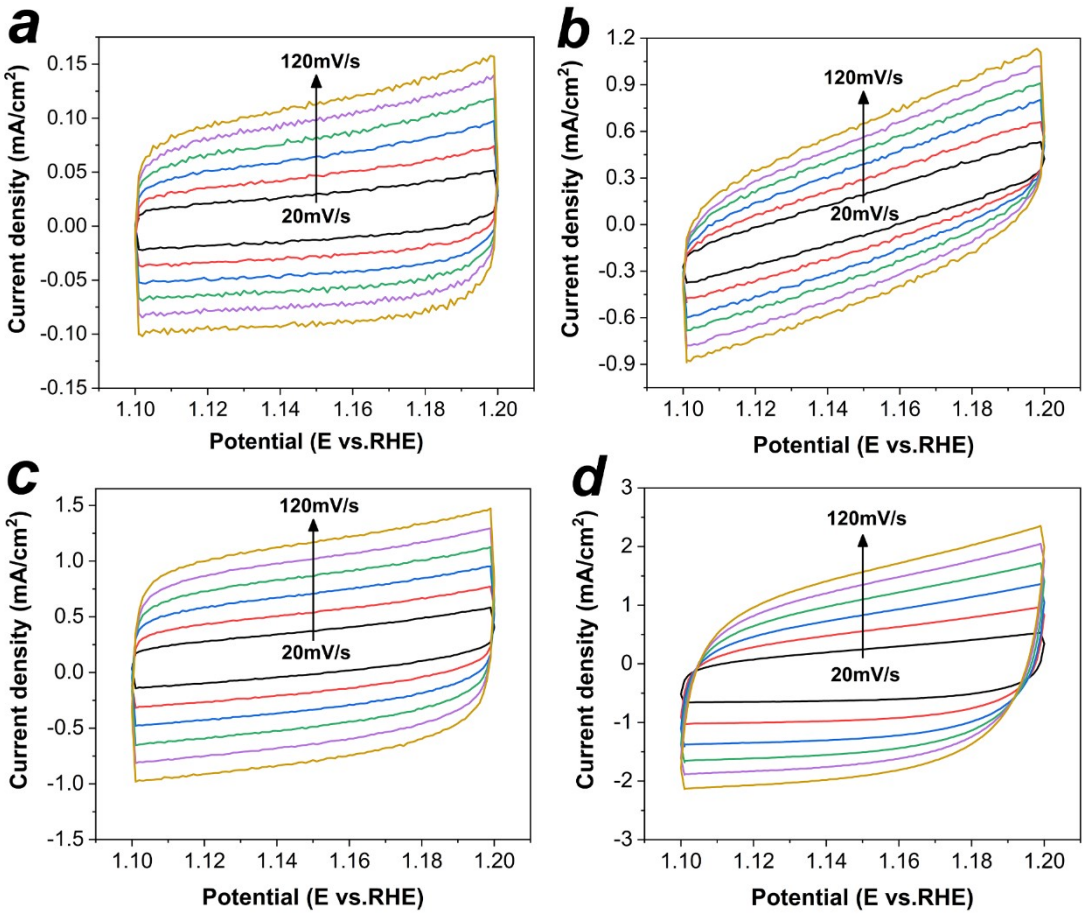

Figure S13 Cyclic voltammetry scans over (a) NF; (b) NiFe LDH@NF; (c) Ni_xSe_y@NF and (d) Ni_xSe_y-NiFe LDH@NF with different scan rates in the non-Faraday region.

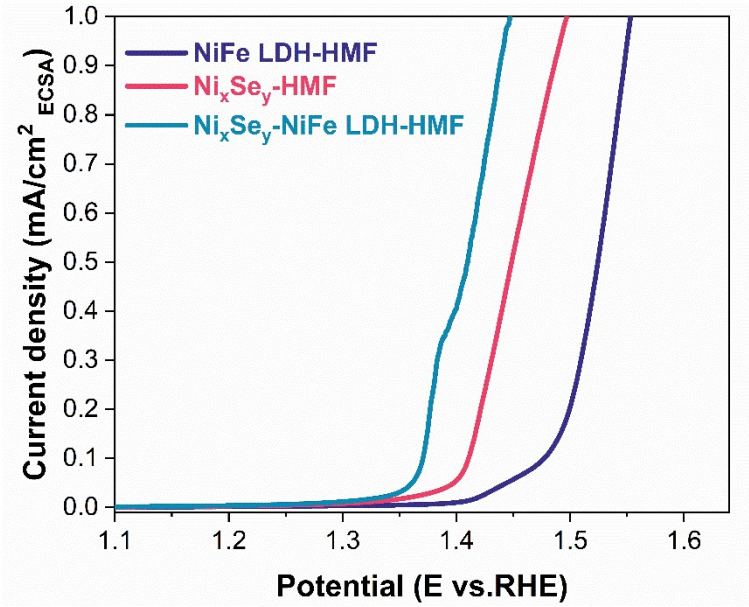

Figure S14 LSV curves with current density normalized by the calculated ECSA of the different catalysts for HMF oxidation.

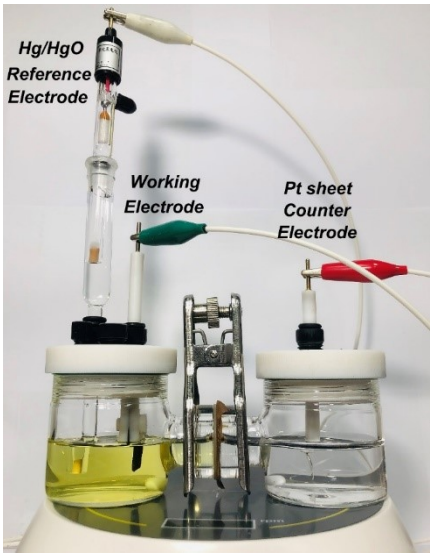

Figure S15 Digital photograph of the three-electrode cell device used for electrochemical oxidation of HMF and FUR.

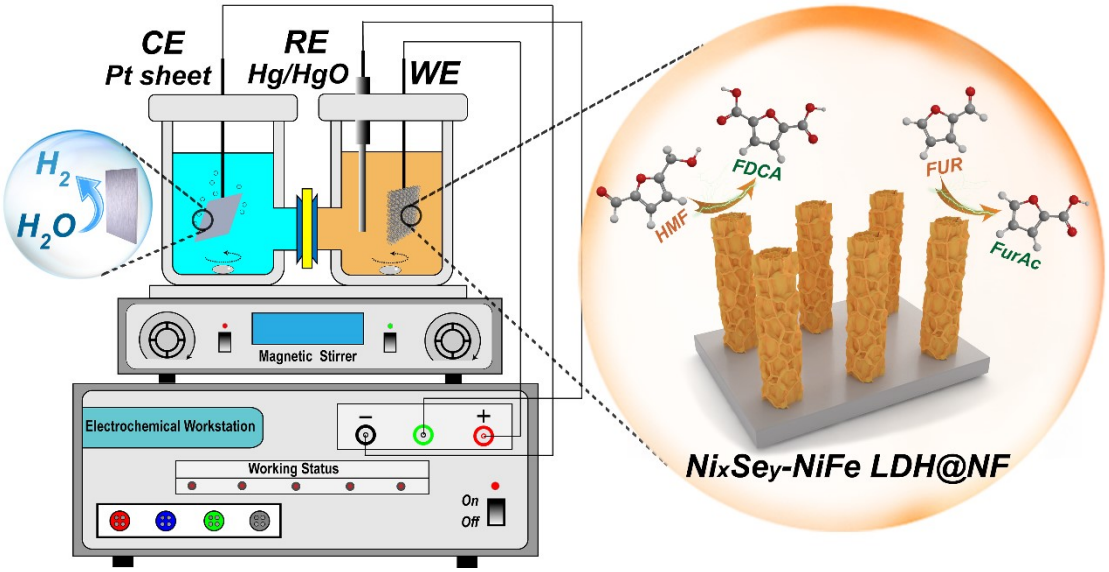

Figure S16 Schematic illustration of the electrochemical device used for electrochemical oxidation of HMF and FUR.

The anode, cathode, and overall reactions for HMF electrochemical oxidation

Anode reaction: $HMF + 6OH^- \rightleftharpoons FDCA + 4H_2O + 6e^-$ (1)

Cathode reaction: $6H_2O + 6e^- \rightleftharpoons 3H_2 + 6OH^-$ (2)

Overall reaction：$HMF + 2H_2O \rightleftharpoons FDCA + 3H_2$ (3)

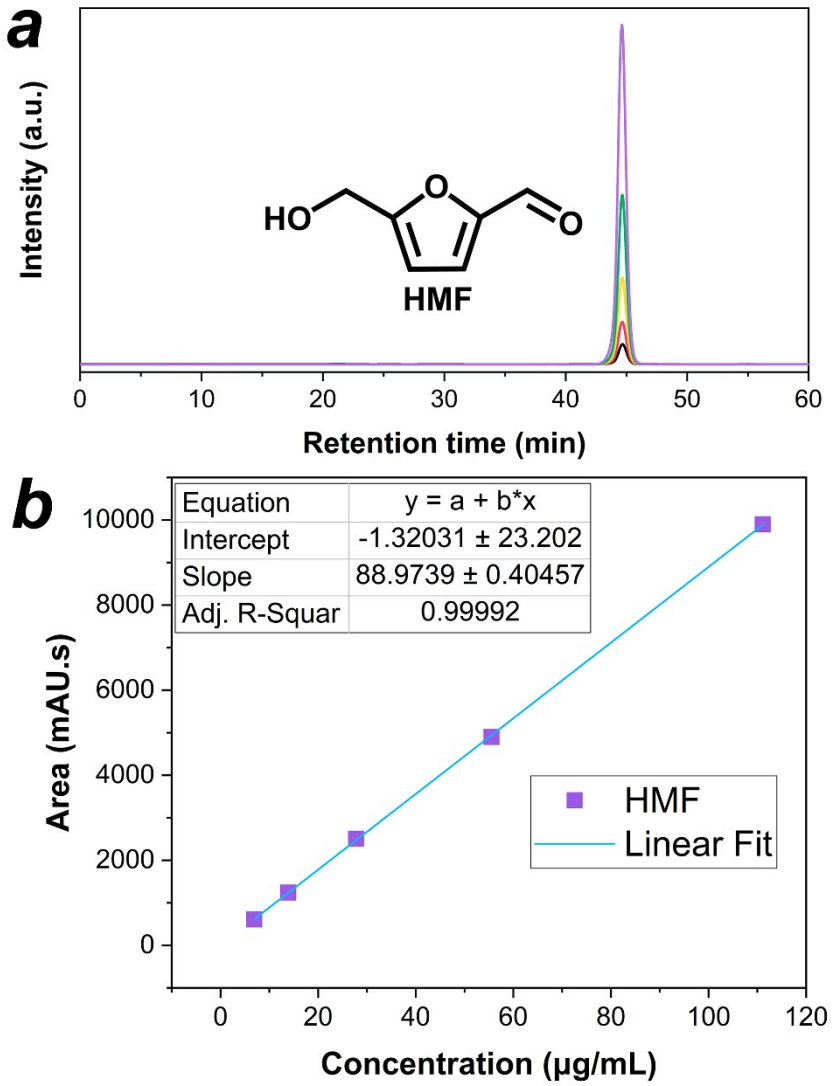

Figure S17 HPLC spectra for (a) standard product of HMF and (b) corresponding calibration curve.

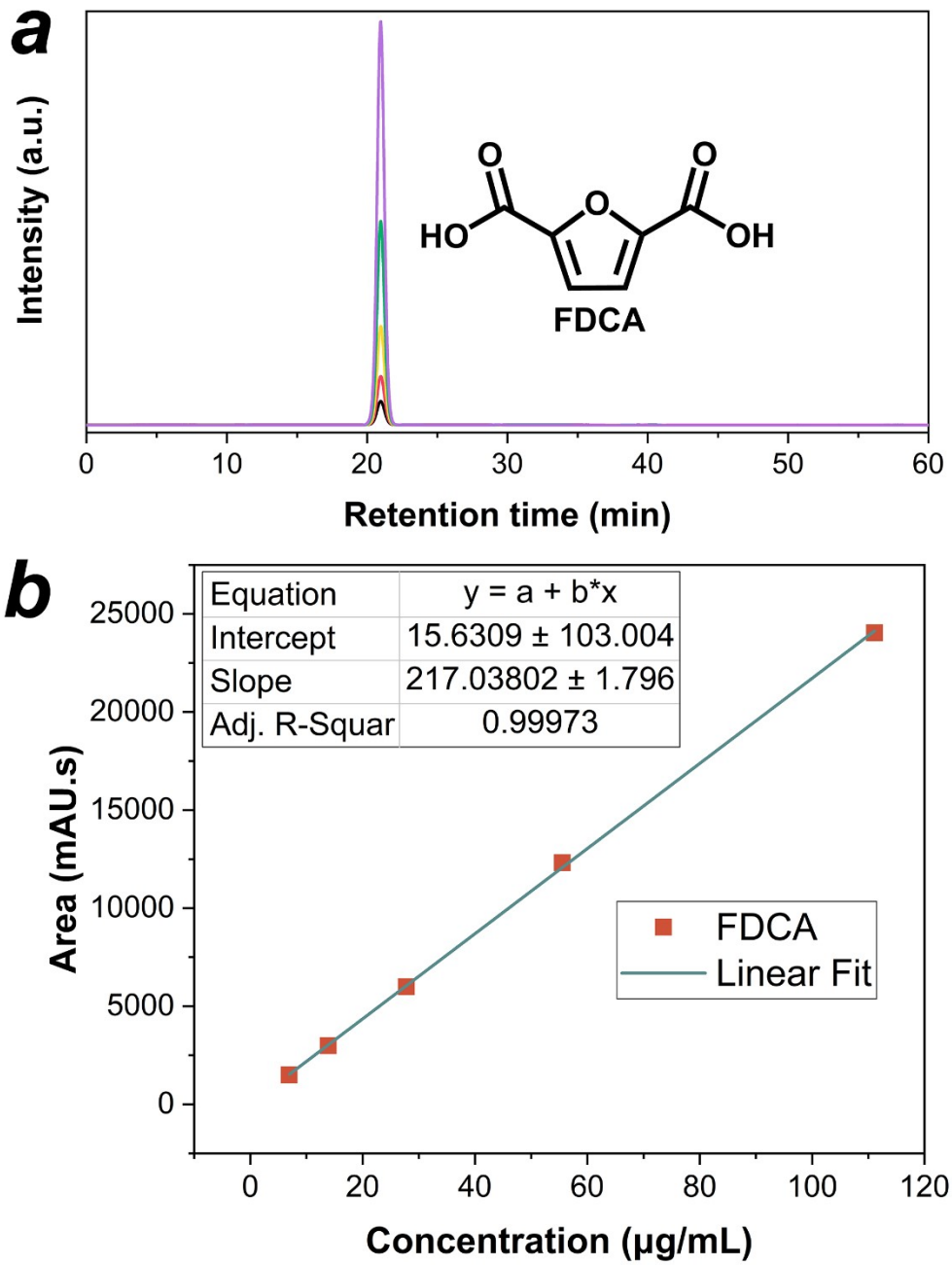

Figure S18 HPLC spectra for (a) standard product of FDCA and (b) corresponding calibration curve.

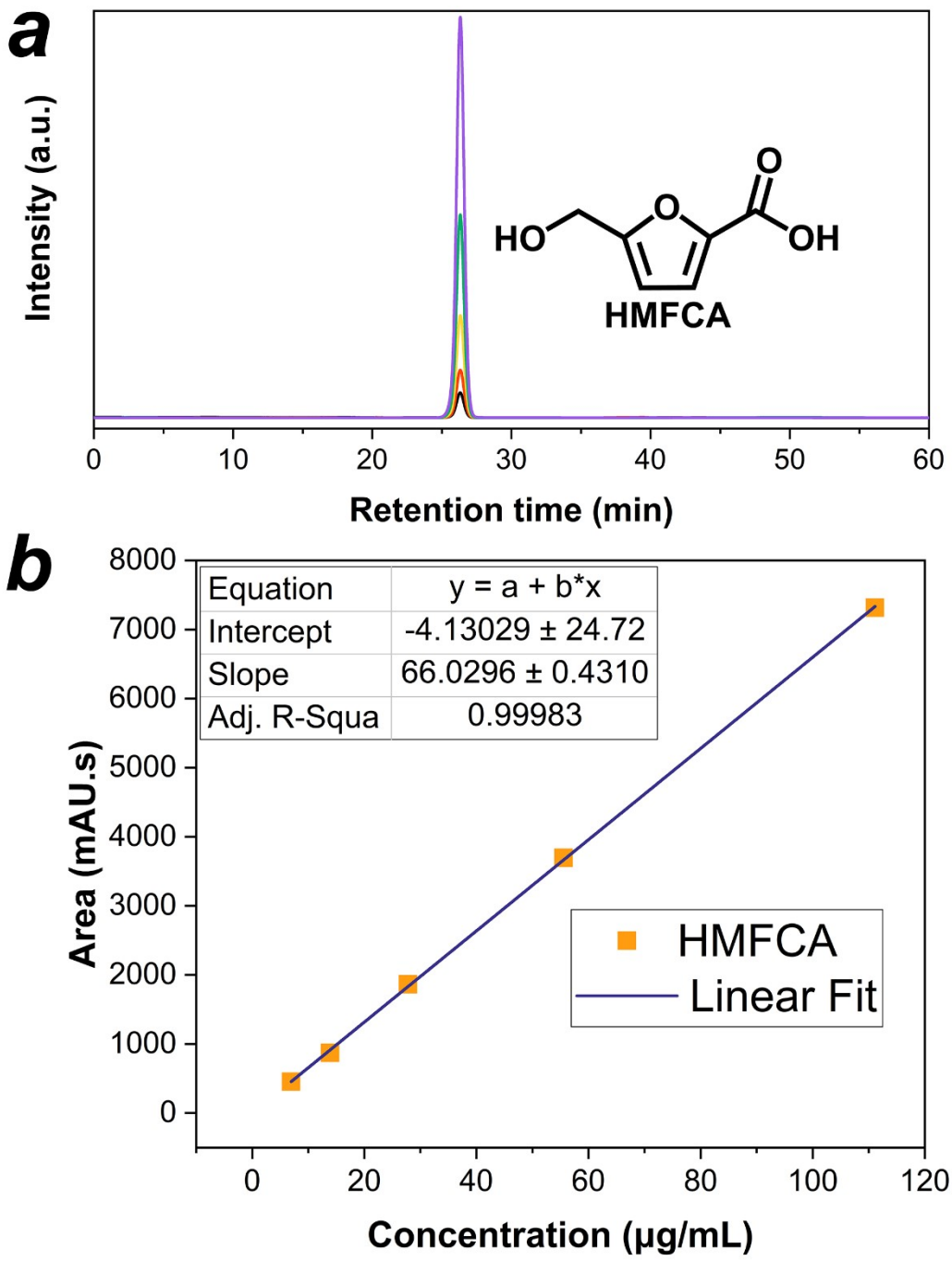

Figure S19 HPLC spectra for (a) standard product of HMFCA and (b) corresponding calibration curve.

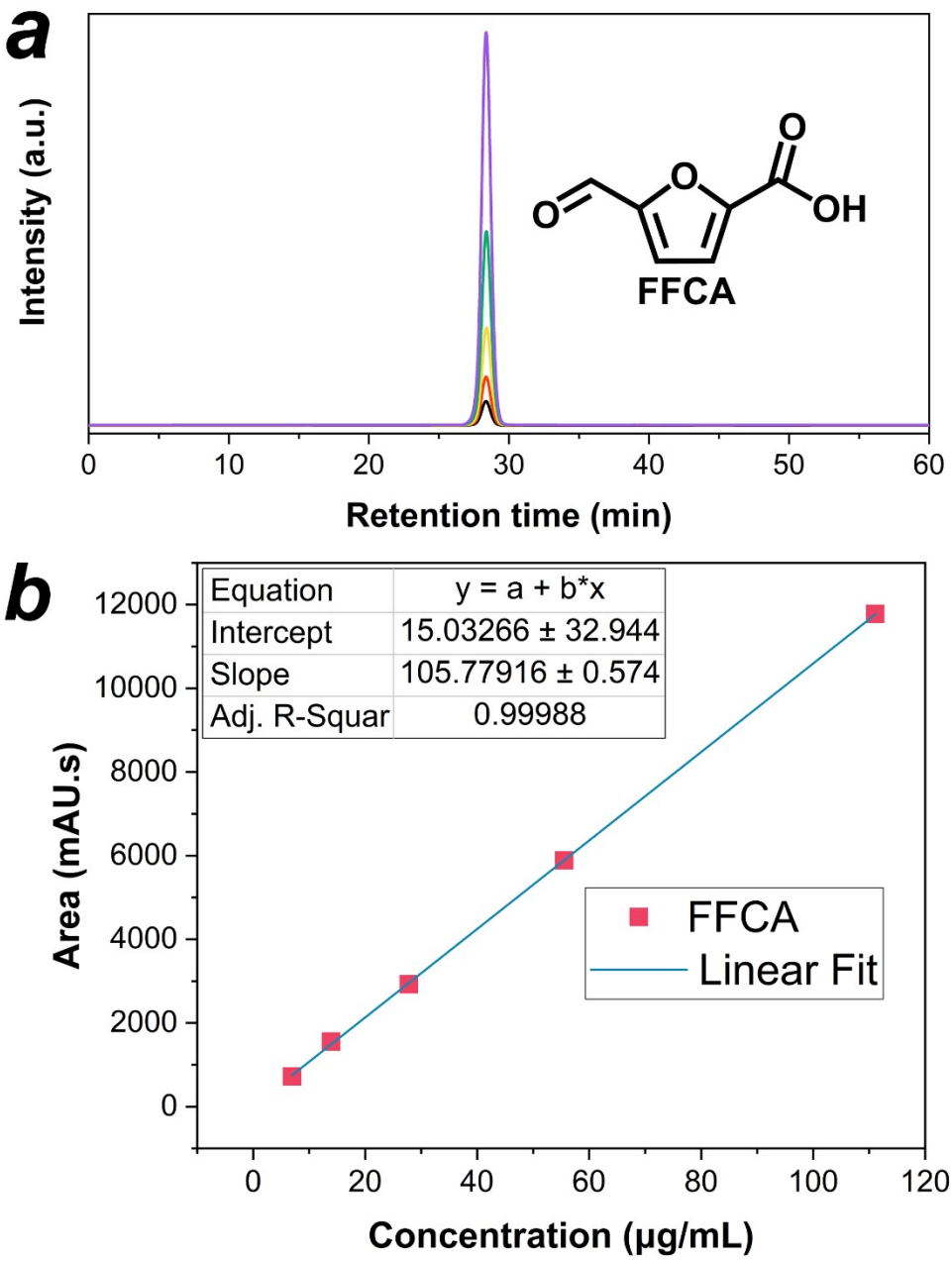

Figure S20 HPLC spectra for (a) standard product of FFCA and (b) corresponding calibration curve.

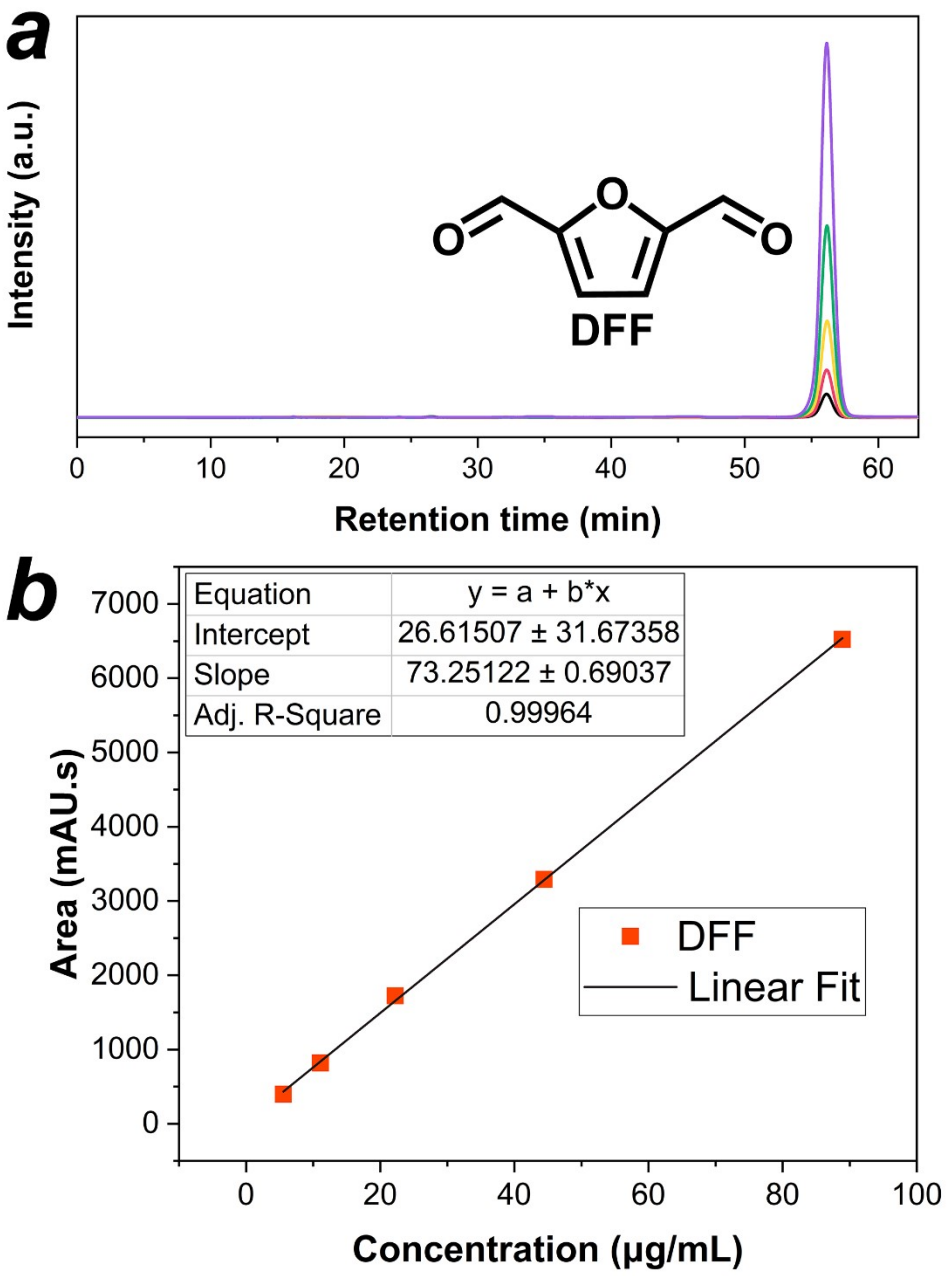

Figure S21 HPLC spectra for (a) standard product of DDF and (b) corresponding calibration curve.

The anode, cathode, and overall reactions for FUR electrochemical oxidation

Anode reaction: FUR + $2OH^-$ ✂ FurAc + H_2O + $2e^-$ (4)

Cathode reaction: $2H_2O$ + $2e^-$ ✂ H_2 + $2OH^-$ (5)

Overall reaction：FUR + H_2O ✂ FurAc + H_2 (6)

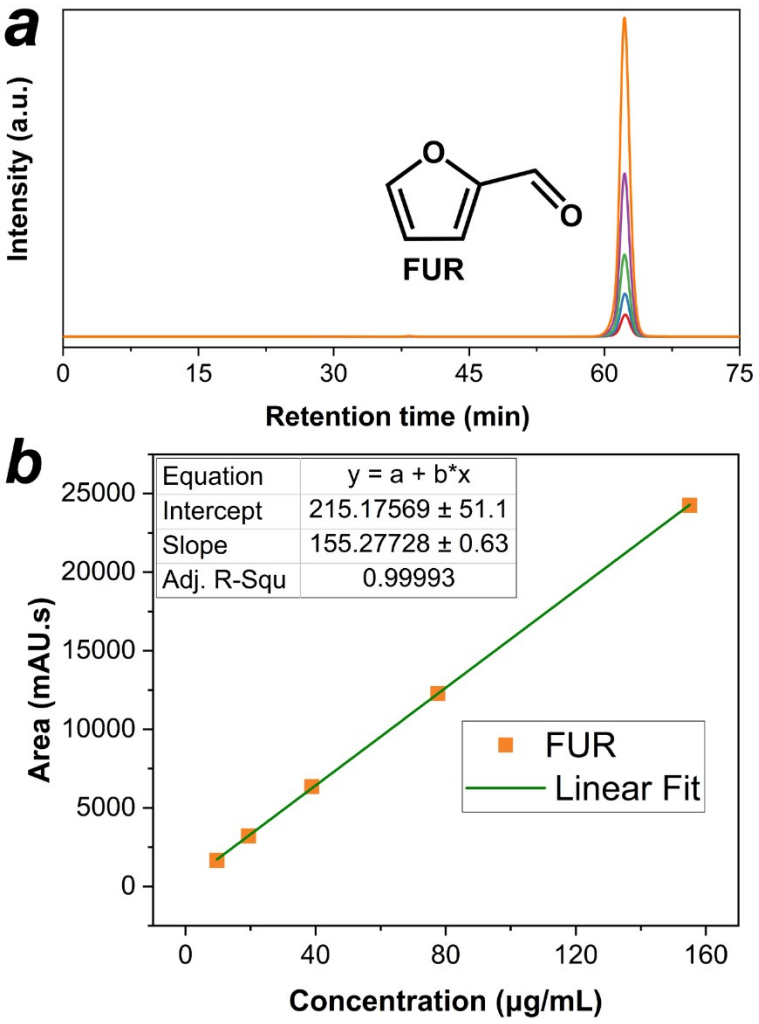

Figure S22 HPLC spectra for (a) standard product of FUR and (b) corresponding calibration curve.

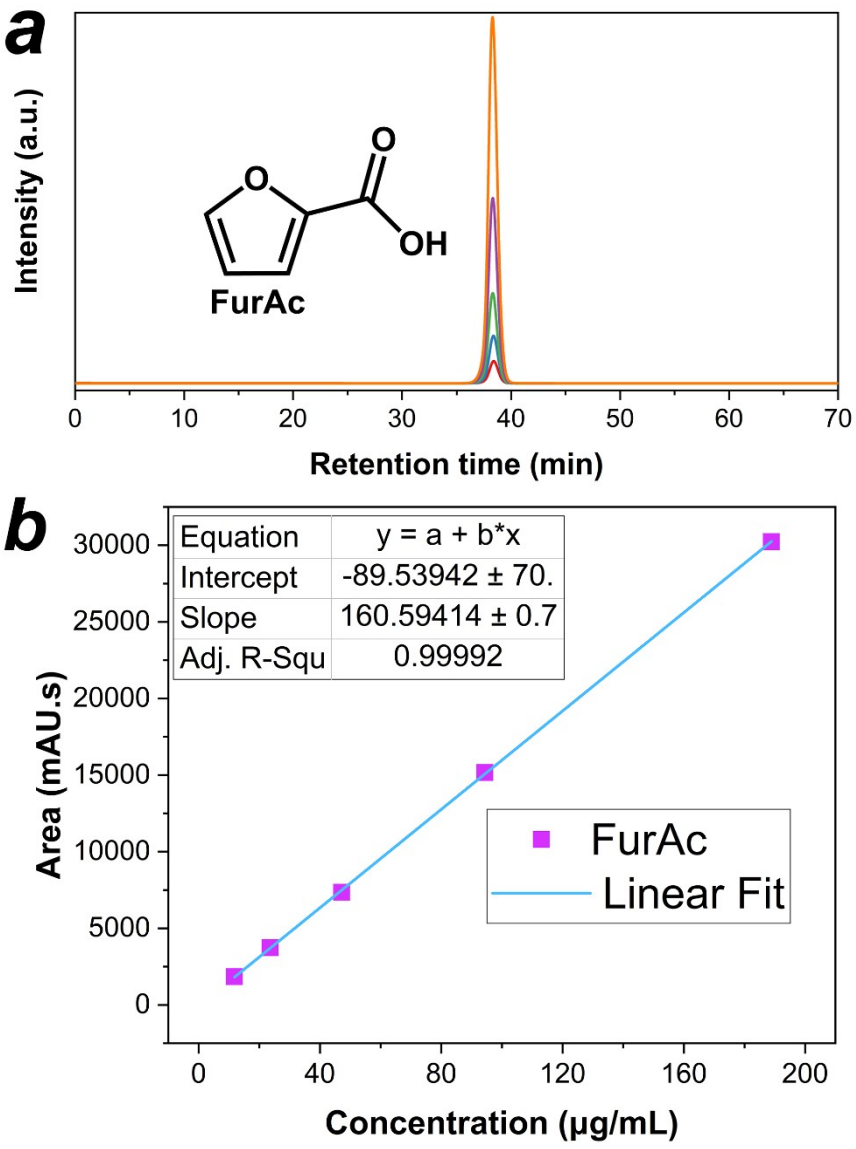

Figure S23 HPLC spectra for (a) standard product of FurAc and (b) corresponding calibration curve.

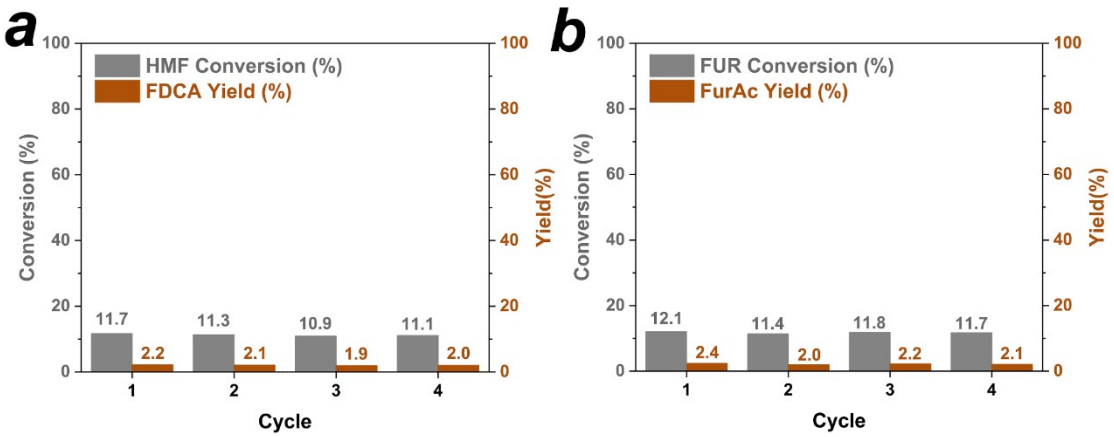

Figure S24 The conversion of and yields towards (a) HMF to FDCA and (b) FUR to FurAc by using NF in four successive electrolysis cycles.

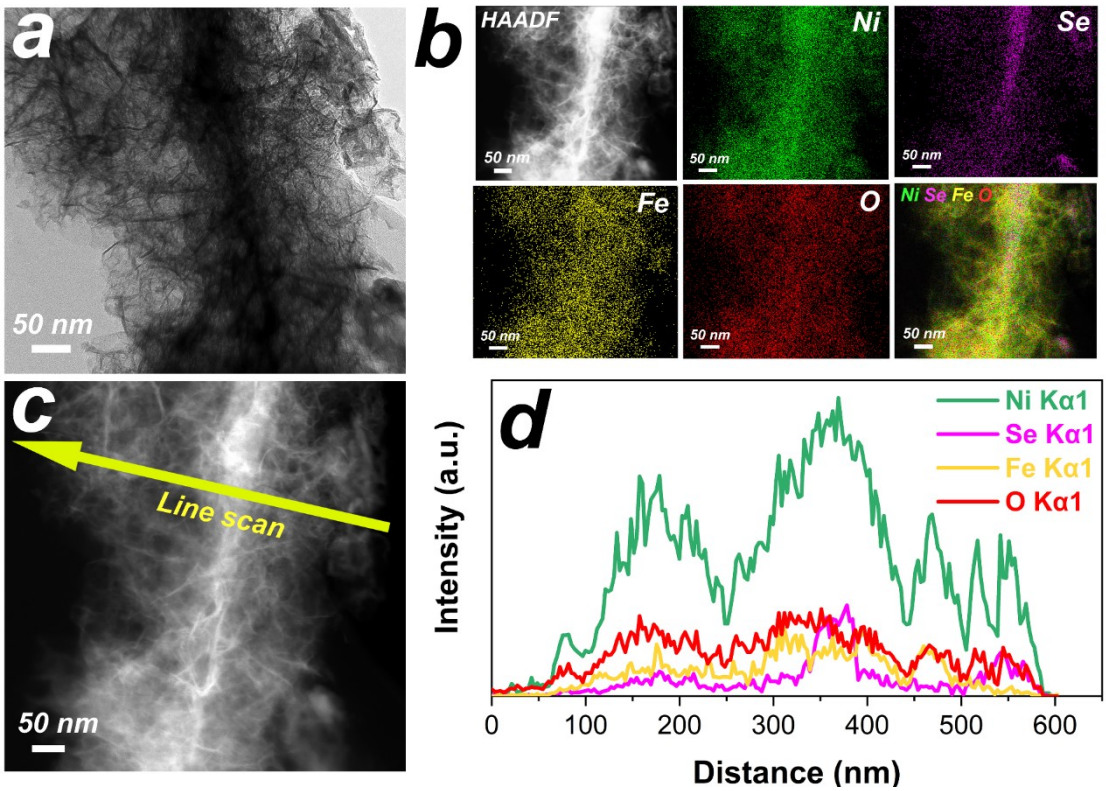

Figure S25 (a) TEM image (b) EDX elemental mapping images and (c,d) TEM line-scan analysis of Ni_xSe_y-NiFe LDH after stability test.

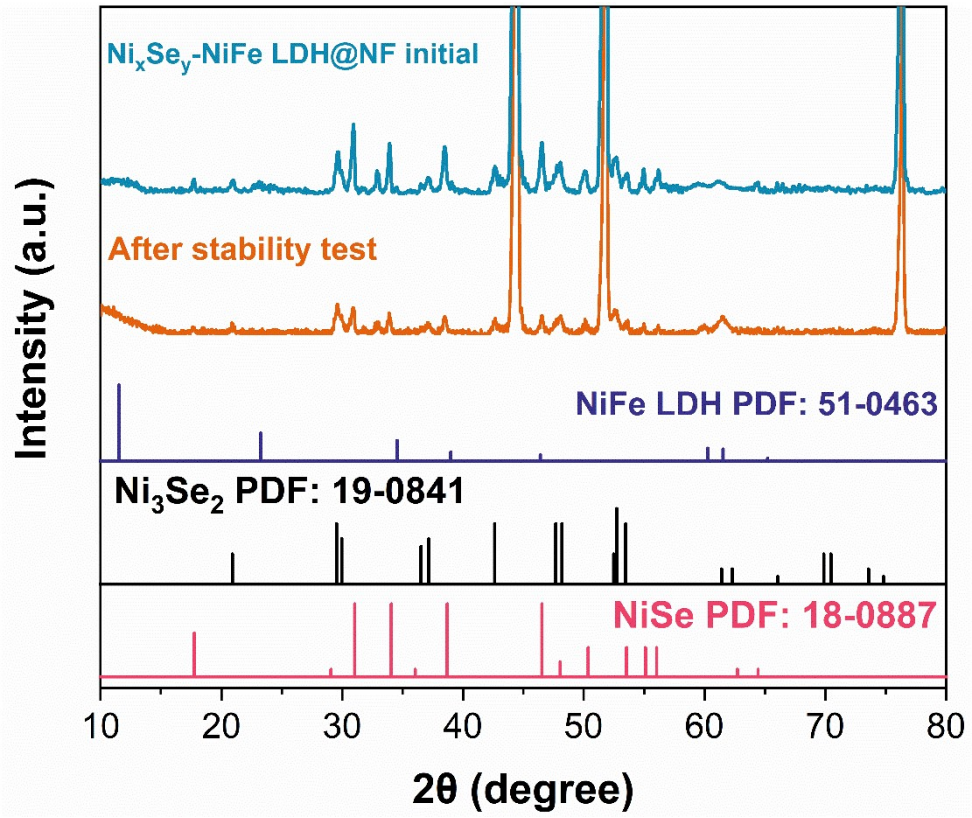

Figure S26 XRD pattern of Ni_xSe_y-NiFe LDH@NF before and after stability test.

Table S1. Comparison of the performance of Ni_xSe_y-NiFe LDH@NF with other reported transition metal-based catalysts towards electrochemical oxidation of HMF to FDCA

Electrode	Electrolyte	Potential Applied	HMF Conversion	FDCA Yield	FE	Cycles	Ref.
Ni_xSe_y-NiFe LDH@NF	1M KOH+10mM HMF	1.423V	99.6%~99.4%	99.3%~97.0%	98.9%~96.7%	6	**This work**
$NiCo_2O_4$@Ni Foam	1M KOH+5mM HMF	1.5V	99.6%~90%	90.8%	87.5%~80%	3	[1]
NiSe@NiO_x	1M KOH+10mM HMF	1.423V	100%~98%	99%~93%	100%~98%	6	[2]
NiFe LDH-CFP	1M KOH+10mM HMF	1.33V	98%~93%	98%	98.6%	4	[3]
NiCoFe LDHs/CFP	1M NaOH+10mM HMF	1.52V	95.5%	84.9% of Selectivity	90%	1	[4]
NiB_x-$P_{0.07}$	0.1M KOH+10mM HMF	1.464V	99.9%~99.9%	90.6%~88.7%	92.5%	3	[5]
$CuCo_2O_4$	1M KOH+50mM HMF	1.45V	Not mentioned	93.7%	94%	6	[6]
Cu_xS@NiCo-LDHs	1M KOH+10mM HMF	1.32V	Not mentioned	~99%	~99%	5	[7]
CoO-$CoSe_2$	1M KOH+10mM HMF	1.43V	~100%	99%	97.9%	5	[8]
Ni_3N@C	1M KOH+10mM HMF	1.45V	Not mentioned	~98%	~99%	6	[9]

Table S2. Comparison of the performance of Ni_xSe_y-NiFe LDH@NF with other reported electrocatalysts towards electrochemical oxidation of FUR to FurAc

Electrode	Electrolyte	Applied Potential or Current	FUR Conversion	FurAc Yield	FE	Cycles	Ref.
Ni_xSe_y-NiFe LDH@NF	1M KOH+20mM FUR	1.423V	99.7%~99.1%	99.7%~97.3%	99.5%~97.1 %	6	**This work**
Ni_2P/Ni/NF	1M KOH+30mM FUR	1.423V	98%	98%~96%	~100%	3	[10]
Ni_2P/CFC	1M KOH+50mM FUR	~1.4V	Not mentioned	~100%	99%~95%	3	[11]
NiCoMn-LDHs/NF	1M NaOH+1mM FUR	1.5V	96.8%~90%	92.4%~85%	~70%	4	[12]
NiGF	1 M NaCl+NaOH+ LiOH + 10% (w/w) FUR	I_{app}/I_{th} = 1.3	87%	83%	Not mentioned	1	[13]
Ni	carbonate buffer +50mM FUR	0.8mA/cm^2	Not mentioned	80%	Not mentioned	1	[14]
Au	carbonate buffer +35mM FUR	0.15V$_{(SCE)}$	56%	95% of Selectivity	Not mentioned	1	[14]

References:

1. M. J. Kang, H. Park, J. Jegal, S. Y. Hwang, Y. S. Kang and H. G. Cha, *Appl. Catal., B*, 2019, **242**, 85-91.
2. L. Gao, Z. Liu, J. Ma, L. Zhong, Z. Song, J. Xu, S. Gan, D. Han and L. Niu, *Appl. Catal., B*, 2020, **261**, 118235.
3. W.-J. Liu, L. Dang, Z. Xu, H.-Q. Yu, S. Jin and G. W. Huber, *ACS Catal.*, 2018, **8**, 5533-5541.
4. M. Zhang, Y. Liu, B. Liu, Z. Chen, H. Xu and K. Yan, *ACS Catal.*, 2020, **10**, 5179-5189.
5. X. Song, X. Liu, H. Wang, Y. Guo and Y. Wang, *Ind. Eng. Chem. Res.*, 2020, **59**, 17348-17356.
6. Y. Lu, C.-L. Dong, Y.-C. Huang, Y. Zou, Z. Liu, Y. Liu, Y. Li, N. He, J. Shi and S. Wang, *Angew. Chem., Int. Ed.*, 2020, **59**, 19215-19221.
7. X. Deng, X. Kang, M. Li, K. Xiang, C. Wang, Z. Guo, J. Zhang, X.-Z. Fu and J.-L. Luo, *J. Mater. Chem. A*, 2020, **8**, 1138-1146.
8. X. Huang, J. Song, M. Hua, Z. Xie, S. Liu, T. Wu, G. Yang and B. Han, *Green Chem.*, 2020, **22**, 843-849.
9. N. Zhang, Y. Zou, L. Tao, W. Chen, L. Zhou, Z. Liu, B. Zhou, G. Huang, H. Lin and S. Wang, *Angew. Chem., Int. Ed.*, 2019, **58**, 15895-15903.
10. N. Jiang, X. Liu, J. Dong, B. You, X. Liu and Y. Sun, *ChemNanoMat*, 2017, **3**, 491-495.
11. X. Zhang, M. Han, G. Liu, G. Wang, Y. Zhang, H. Zhang and H. Zhao, *Appl. Catal., B*, 2019, **244**, 899-908.
12. B. Liu, S. Xu, M. Zhang, X. Li, D. Decarolis, Y. Liu, Y. Wang, E. K. Gibson, C. R. A. Catlow and K. Yan, *Green Chem.*, 2021, **23**, 4034-4043.
13. G. Chamoulaud, D. Floner, C. Moinet, C. Lamy and E. M. Belgsir, *Electrochim. Acta*, 2001, **46**, 2757-2760.
14. P. Parpot, A. P. Bettencourt, G. Chamoulaud, K. B. Kokoh and E. M. Belgsir, *Electrochim. Acta*, 2004, **49**, 397-403.